Chapter

Significance of Mesoscale Warm Core Eddy on Marine and Coastal Environment of the Bay of Bengal

Nanda Kishore Reddy Busireddy, Kumar Ankur and Krishna Kishore Osuri

Abstract

Bay of Bengal (BoB) is an affluent region for the mesoscale (eddies) and synoptic scale (cyclones) systems. It occurs primarily through the seasonal variations, dynamical instabilities and equatorial wind forcing mechanisms. The individual or cumulative effect of these changes is vulnerable to the coastal and marine ecosystems. For example, tropical cyclone (TC) AILA experienced a warm core eddy (WCE) before the landfall, and consequently it intensified into a severe cyclonic storm (CS) and remained as a CS up to 15 h after the landfall. Its severity produces a heavy rainfall of >18 cm day^{-1}, thus leads to the coastal flooding. The eddy contribution to the TC is witnessed during and after the landfall. Inappropriately, high resolution *in-situ* observations are not available to identify such important processes on different time and spatial scales. Therefore, the present chapter analyses the northern BoB eddy induced signals using both *in-situ* and satellite (advanced microwave scanning radiometer—AMSR-2) derived products. Two *in-situ* locations (BD08 and BD09) are employed for this study purpose. The eddy responses at no-eddy, during and after eddy, have been analyzed. Besides, WCE imprints on the overlying atmosphere are also observed. The relationship between sea surface temperature and wind speed over the BoB region is assessed.

Keywords: warm core eddy, tropical cyclone, *in-situ*, AMSR-2, sea surface temperature, wind speed

1. Introduction

Marine environment usually influences or is influenced by the mesoscale (eddies) and synoptic scale (cyclones) processes. The horizontal scale of a typical mesoscale eddy is varying in between 100 and 200 km with a lifetime of 10–100 days [1–3]. The preserved shape carries/responsible for the mass or heat transport, turbulent current patterns, thermodynamic properties, potential fishing zones and upwelling processes over a long distance [3, 4]. Oceanic mesoscale eddies are of two types such as warm and cold core eddies. The significance of the warm (cold) core eddy is that it contains a higher (lower) temperature with elevated (lower) sea level in the center. The primary factors responsible for the genesis of the eddies were force exerted by the wind stress curl, meander separation, baroclinic instability and gradient wind balance [5]. Mesoscale eddies play an important role in

governing the atmospheric vortices such as tropical cyclones (TCs) and ultimately affect its intensity. For example, cold core eddy promotes TC weakening while, warm core eddy (WCE) amplifies the TC intensity. It is known fact that the coastal and marine environments are sensitive to such oceanic vortices.

The Bay of Bengal (BoB) is an eddy rich region and is located in the northeastern part of the Indian Ocean (**Figure 1a**). The location of the BoB in the global and regional prospective is shown in the **Figure 1a**. It is dominated by the several factors such as freshwater discharge, seasonal occurrence of storms, monsoonal reversal winds and upwelling plumes [6, 7]. All these factors contribute to the formation of eddies throughout the year in this bay. The persistent eddy environmental characteristics determine the weather of the ocean and its overlying atmosphere. For example, ocean heat content is considered to be an important parameter in the ocean perspective that can modulate the atmospheric vortices [8, 9]. In case of WCE, the preserved heat content provides the sufficient positive energy to the storm in terms of large enthalpy fluxes and thus helps in the intensification process. Similarly, the process is opposite in case of cold core eddy. Moreover, it also has a
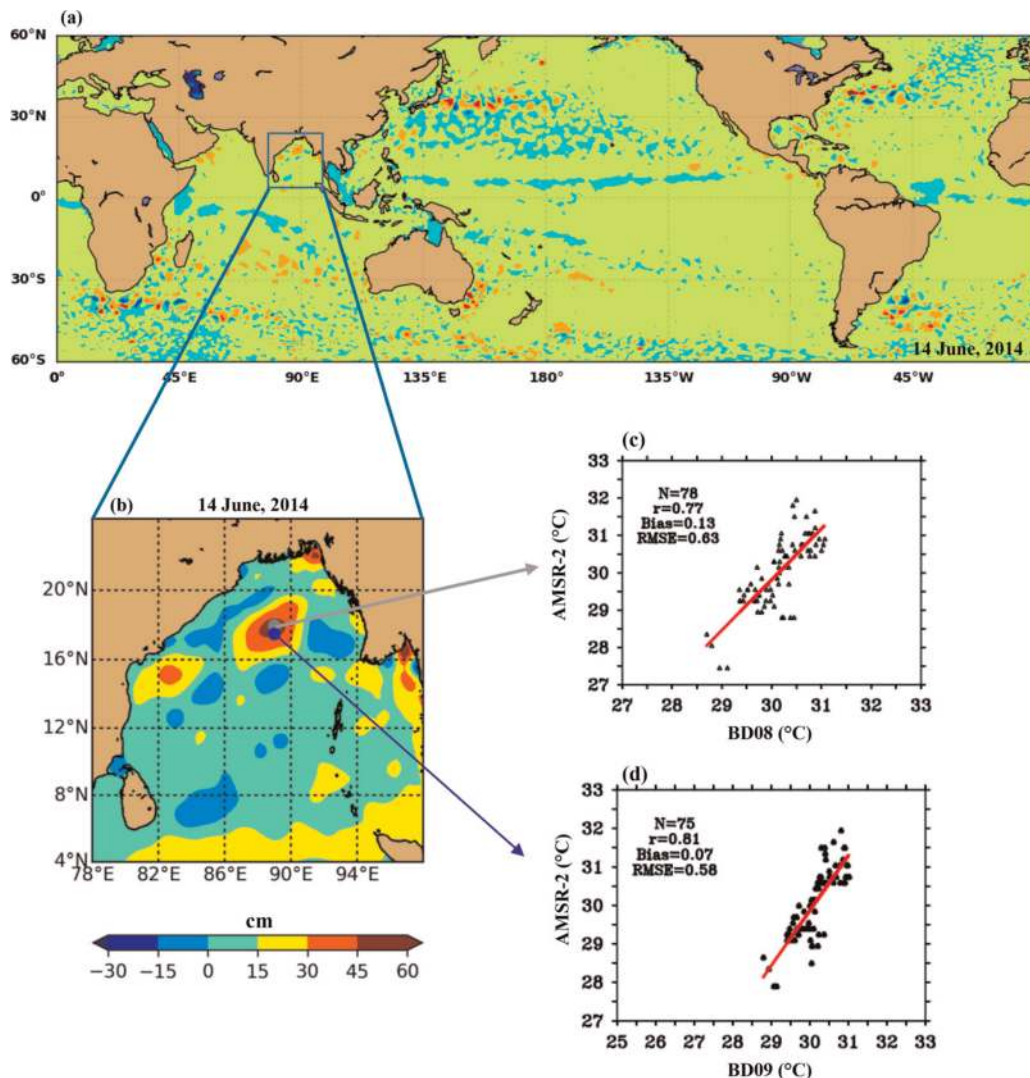

Figure 1.
Sea level anomaly of (a) global oceans, on 14 June 2014. The blue rectangle represents the zoomed version of (b) Bay of Bengal showing the warm core eddy. (c and d) The statistical analysis of sea surface temperature (°C) between AMSR-2 satellite and BD08 and BD09 observations during the eddy period (05 May–25 July 2014). Gray and blue color circles in (b) shows the BD08 and BD09 moorings.

major implication, when the WCE forms in the close proximity of the coastal region and a storm passes over on it. It poses a major socioeconomic impact on the coastal communities, agriculture and infrastructure, thus ultimately lead to the catastrophic damage. A best example related to this situation is TC Aila (2009) over the BoB. According to Regional Specialized Meteorological Center report (2010) and Sadhuram et al. [10], TC Aila suddenly gets intensified by 43% within a day before the landfall and caused for the 175 human deaths. These kind of similar events have been noticed around the global oceans. For example, Hurricane Opal (1995) in the North Atlantic Ocean and Super Typhoon Maemi (2003) in the western North Pacific under-went a WCE, and shows a sudden rapid intensification within a 24–36 h-time window [11, 12]. The principle behavior of these WCEs is that it acts like an insulating material against the ocean waters negative feedback and boost the TC intensity process [13]. While, it is true for cold core eddies thus provides a negative feedback to the storm and finally it gets weakens. However, there are other positive impacts associated with these cold core eddies that indirectly help the marine processes. It actually brings the subsurface chlorophyll maxima to the surface area and turn it into higher biological productivity in that region [14]. The detection of these eddies using the sea surface temperature (SST) gradient patterns is a difficult task because the attained surface variations are less. The better approach to deal with these mesoscale eddies are using the altimeter derived sea level anomalies (SLA) in which the high and the low SLA signal gives an indication of warm and cold core eddies [5].

Over the decade, understanding of these mesoscale eddy variability in the spatial and temporal manner has got a steady improvement. Bruce et al. [15] reported the mesoscale eddy features using the TOPEX altimeter data. Frenger et al. [16] analyzed the impact of these eddies on the atmospheric parameters such as winds, clouds and rainfall. Dandapat and Chakraborty [17] analysed the three dimensional structure of the mesoscale eddies using both the altimetry and Argo floats for the period 1993–2014. Busireddy et al. [18] shows the thermohaline structures associated with the WCE and its response on the overlying atmosphere. Despite these facts, the eddy-resolving models are still lacking to capture the realistic features of the ocean tractable in the BoB region. In summary, mesoscale eddies and its feedback to the atmospheric vortices suggest the urgency of high resolution ocean-atmosphere coupled models and satellite products over the region.

The present chapter is evolved by considering the availability of the existent high-resolution *in-situ* (buoy) and remote sensing (satellite derived) products and addresses the eddy induced signals in the ocean and atmospheric parameters. The overall discussion is followed primarily by choosing the (1) WCE during the normal conditions and in the presence of a cyclone environment, (2) sea surface temperature (SST) and wind speed data products verification of advanced microwave

Parameter	Sensor type	Resolution	Accuracy	Range
In-situ SST	Thermistor/Seabird Micro-CAT SBE37	0.0001°C	0.002°C	−5 to 35°C
In-situ wind speed	Vane + flux gate compass/ Lambrecht	0.1 ms^{-1}	±2%	0 to 35 ms^{-1}
AMSR-2 SST	Microwave radiometer	$0.25° \times 0.25°$	±0.8°C (released)	−2 to 35°C
AMSR-2 wind speed			$±1.5 \text{ ms}^{-1}$ (released)	0 to 30 ms^{-1}

Table 1.
Specifications of SST (°C) and wind speed (ms⁻¹) parameters of both in-situ and AMSR-2 sensors.

scanning radiometer (AMSR-2) over the BoB region and (3) SST-wind speed relationships during the WCE, near coastal region and open oceans using satellite and *in-situ* measurements. This study signifies the inevitability of high resolution products in the coastal and marine environments over the BoB. The resolution and accuracy of the satellite and *in-situ* products is demonstrated in **Table 1**. The buoys (BD08 and BD09) collects both the surface met and ocean parameters with depth. The thermohaline features are nearly similar at both the locations before and after the warm core eddy period. However, significant differences are seen during warm core eddy period owing to its spatial variation. The vertical thermohaline structures exhibited ridge and trough structures throughout the eddy life. It is worthwhile to note that the structures are prominent during developing stage of warm core eddy, however, they are nearly uniform in the weakening phase of warm eddy. More details on the eddy induced signals before, during and after the warm core eddy can be obtained from Busireddy et al. [18].

2. North Bay of Bengal

The Bay of Bengal is surrounded by India (in the west and northwest side), Bangladesh (in the north), Myanmar and the Andaman/Nicobar Islands of India (in the east) and Sri Lanka (in the south) (**Figure 1a**). A number of major rivers belonging to the India, Bangladesh and Myanmar is flowing into the northern BoB. In the tropics, Northern BoB has a unique feature among the world as it is dominated by the low surface salinity due to seasonal reversal of the monsoon winds, freshwater discharge from the major rivers and the seasonal occurrence of cyclones [19]. During the summer monsoon season (June-September), northern BoB is conducive for the several meteorological systems that brings rainfall to the central and Northern parts of India. Alike, the massive river outflow, which is coupled with rainfall eventually drain into the bay region. These large supplies of fresh water and rainfall resulting in the strong near surface layer stratification led to the formation of the barrier layer. Likewise, during winter season (November-December), the region experiences a strong surface layer temperature inversion due to the sustained salinity stratification of the summer monsoon. Moreover, the region is active for the mesoscale eddies that are formed due to the active coastal upwelling Kelvin wave during the spring intermonsoon period (March-May) [18, 20].

2.1 Warm core eddy

A warm core eddy has been identified using the spatial maps of sea level anomalies (SLA) obtained from the Archiving, Validation, and Interpretation of Satellite Oceanographic (AVISO) over the northern BoB (**Figure 1b**). It is noted that the size of the eddy is around 5° × 5°. Chelton et al. [21] criteria are applied for the eddy identification purpose and realized that it is centered at around 89°E and 18°N with a life period of 3 months (05 May 2014–25 July 2014) in the northern BoB. The eddy was surrounded by the several alternative warm and cold core rings (**Figure 1b**). The further details regarding the genesis and its propagation characteristics are demonstrated in Busireddy et al. [18]. In general, the eddy size is often associated with the Rossby radius of deformation which is increased from higher to lower latitudes. It is termed as the length scale at which rotational effects become equally important as the buoyancy or gravitational effects in a flow field. From Figure 3b of Chen et al. [22], the Rossby radius of deformation values are 60 km at 20°N and 130 km at 9°N. Incidentally, two of the moored buoys (BD08 and BD09), deployed earlier by National Institute of Ocean Technology, are located within the eddy

region. The buoys provide the incessant time series measurements of ocean temperature and salinity profiles. Therefore, the estimated Rossby radius (L = NH/f) at 18°N latitude using the buoy observations is 39 km and is consistent with Chen et al. [22]. Here, N is the Brunt-Vaisala frequency ($0.0179\ s^{-1}$), H is the scale height or equivalent depth (100 m), and f is Coriolis frequency ($4.505 \times 10^{-5}\ s^{-1}$). According to the Space Application Centre, Indian Space Research Organization (ISRO), India (https://www.mosdac.gov.in/oceanic-eddies-detection), the radius of the present eddy derived from AVISO data is ~170 km. The fact to be noted that the eddy radius (~170 km) is much bigger than the Rossby radius (39 km) means that there are some other effects contributing to this large-scale eddy formation.

The statistical analysis of SST between the *in-situ* and AMSR-2 is carried out at two moored buoy locations in the northern BoB (BD08 at 89°E/18°N and BD09 at 89°E/17.5°N) to quantify the uncertainty of the satellite derived SST in the presence of WCE (**Figure 1c** and **d**). The AMSR-2 data description and its validation information are made available online at http://www.remss.com/missions/amsr/. Considering the surface ocean temperatures, the buoys observed an unusual increase of 3–4°C during the WCE period. In order to capture these kinds of similar variations using the satellite, primarily, the capability of the AMSR-2 SST is verified with respect to the BD08 and BD09 during the eddy period. The statistical analyses show a root mean square error (RMSE) of 0.5–0.6°C at both the buoy locations. The correlation and bias are varying in between 0.7–0.8 and 0.07–0.13°C, respectively (**Figure 1c** and **d**). As stated in Reddy et al. [23], the AMSR-2 mean SST error over the BoB is limited to ~0.3°C. In this situation, the observed RMSE (~0.5–0.6°C) in the WCE period is doubled as that of mean RMSE (~0.3°C) over the BoB. It infers that AMSR-2 SST shows a large error in the presence of mesoscale eddy. However, these error values are within the satellite prescribed release accuracy range (i.e., ±0.8°C). The results provide that AMSR-2 is over estimating for the higher SST values.

In addition to the ocean responses, the WCE provides it signatures on the surface meteorological variables. The noticeable variations on the surface-air temperature (SAT) and sea-surface temperature (SST) anomalies, air-sea specific humidity values and enthalpy fluxes during the WCE period is observed [18]. During the eddy progression, i.e., from genesis to peak stage, both the SAT and SST anomalies show similar changes and exhibits its peak magnitude of 3°C at the peak stage. In contrast, significant differences have been noticed during the peak-to-dissipation stage. The mean differences between the SAT and SST anomalies are 0.01 and 0.6°C, respectively. These differences indirectly cause for the changes in the surface turbulent fluxes, which is the main source for weather systems (i.e., cyclones). It is observed that the strong air-sea temperature differences in the WCE lead to the sharp increase in the latent heat flux and sensible heat flux of 504 and 142 W m^{-2}, respectively [18]. The comparison of these values with the climatology revealed that the eddy induced fluxes are higher by 274% and 370% [7, 24]. **Table 2** illustrates the estimated values of buoy (BD08) air-sea parameters and its corresponding AVISO SLA values during the eddy evolution. In order to understand clearly, the WCE period is broadly classified into various phases such as no-eddy, genesis, intensifying phase, peak stage, phase and dissipation phase, respectively [18]. The obtained results indicated that for all the parameters, values are increasing beginning from the no-eddy, genesis and reaches to its higher values at the peak stage. Thereafter, it reaches to its normal values during the dissipation stage. For example, the estimated ocean heat content at peak stage shows an increment of 258%, when compared to the no-eddy conditions [18]. Similarly, the other parameters such as wind speed, SST and SLA also exhibits a similar increment of 51, 3.6 and 98%, respectively when compared to that of no-eddy conditions.

2.2 Role of warm core eddy in the intensification of AILA (May 2009) cyclone over BoB

The greatest contributors to the coastal flooding and its associated damage are mainly due to the landfalling cyclones. It is generally formed over the warm waters (>26.5°C) and gains the remarkable amount of energy from the ocean [25]. The typical size of the TCs are 200–2000 km with a time period of 1–2 weeks [26]. Aila is a severe cyclonic storm that formed over the northern BoB and made landfall near the Sagar Island on 25 May 2009. The strong winds and storm surge cause for the 175 human deaths (http://www.rsmcnewdelhi.imd.gov.in). The prominence of cyclone is that it intensified from cyclone to severe cyclonic storm within a few hours before the landfall. The later studies revealed that one of the reasons for sudden intensification is due to the presence of WCE in near at the coastal region of the West Bengal. **Figure 2** shows the AILA cyclone track and its corresponding time series analysis of SLA, cyclone intensity and wind intensity (kt) values. The SLA depicts the occurrence of WCE close proximity to the West Bengal coast. During the Aila cyclone movement, it encountered a WCE on 24 May 2009 as a cyclonic storm and get intensified into a severe cyclonic storm within a short time span. It is observed that WCE maintains an SST of 31°C during the time and favors the storm intensity increase by 43%. The high ocean heat content and deep isothermal warm

Phases/parameters	OHC (kJ cm^{-2})	Wind speed (ms^{-1})	SST (°C)	SLA (cm)
Before/no-eddy	40	4.9	30.0	25.4
Genesis	69	1.4	30.1	26.1
Intensifying phase	109	4.7	30.4	38.3
Peak stage	139	7.4	31.1	50.5
Weakening phase	100	7.2	29.7	35.8
Dissipation stage	7	5.0	28.6	13.7

Table 2.
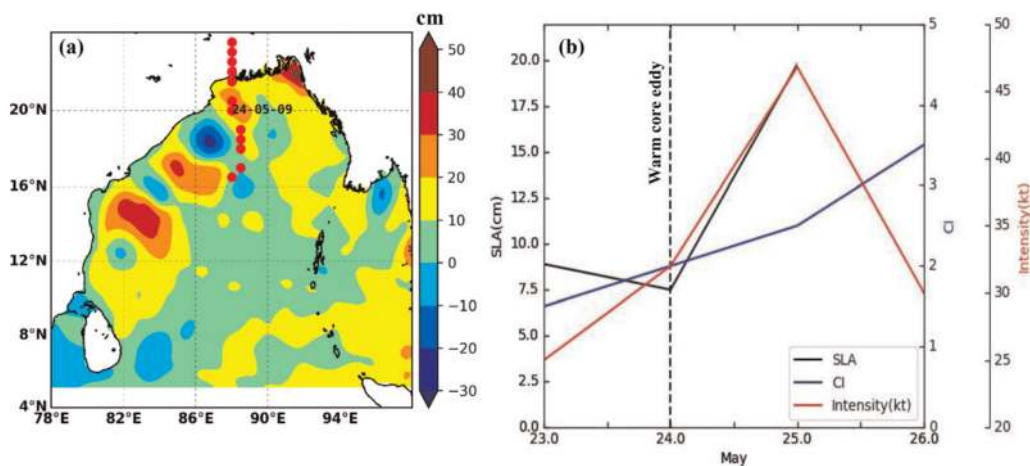*Quantification measures of BD08 atmosphere-ocean parameters during no-eddy to dissipation stages.*

Figure 2.
AILA tropical cyclone passing through the warm core eddy in (a) and its corresponding time series analysis of sea level anomaly (SLA), cyclone intensity (CI) and wind intensity (kt) values along the track shown in (b). Shaded background in (a) and vertical dashed line in (b) represents the SLA and warm core eddy crossing day respectively.
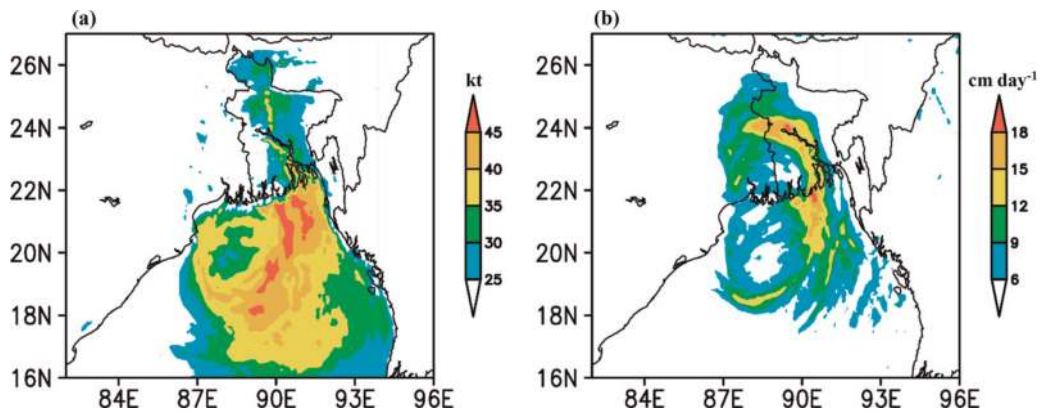
Figure 3.
(a) Maximum sustained wind swath in the life span of the TC AILA (23–26 May 2009) and (b) 24-h accumulated rainfall during landfall day valid at 03 UTC 26 May 2009.

layer within the eddy inhibit the storm induced cooling and further help in the intensification process [10]. From **Figure 2b**, the time series analysis of SLA and wind intensity shows a usual value ranging from 7.5 to 9 cm and 25–32 knots before it arrives into the eddy region. Once the TC encountered the eddy (24 May 2009), SLA shows a sudden increment of 9–20 cm with the corresponding increase in wind intensity from 32 to 47 knots. Sadhuram et al. [10] explained that high SST and large enthalpy fluxes beneath the eddy provides a positive feedback and support to the TC intensification process. Along with this, cyclone intensity also shows a positive trend throughout the TC life period. Moreover, the cyclone made landfall on 25 May 2018 so the SLA is absent and wind intensity values decreases due to the land interaction.

Figure 3 shows the spatial distribution of wind speed and rainfall associated with the Aila cyclone during the landfall. The wind speed was obtained from FiNaL (FNL) analyses of the National Center for Environmental Prediction (NCEP) and the rainfall (3-hourly) from the Tropical Rainfall Measuring Mission. The structural wind swath analyses show a peak wind intensity of >45 knots that persists over the Bangladesh even after the landfall. As mentioned earlier, the presence of WCE during the AILA passage supports its intensification into a severe cyclone, while the abundant soil moisture from the land surface conditions (Delta region of the River Ganga) helps to sustain/maintain the intensity for next 15 h. The analysis from the spatial distribution of 24-h accumulated rainfall during the landfall exhibits a high rainfall of ~15–18 cm day^{-1}. Moreover, these rainfall are elongated to a few hundred kilometers away from the coast. The down-pouring of heavy rain in some places around the Sundarban area lead to the coastal inundation and flooding. According to the India Meteorological Department, New Delhi, a storm surge of ~3 m is experienced in the western regions of Bangladesh and it is 2–3 m over the Sundarban area region (http://www.rsmcnewdelhi.imd.gov.in).

3. SST and wind speed analysis over the BoB

As we know that SST is a vital parameter in the coastal and marine environment that can regulate both the physical and biological processes. The SST changes are directly associated with the magnitude of the wind speed. Higher (lower) the magnitude lower (higher) the SST values. Here, the performance of the AMSR-2 SST and wind speed is verified at two *in-situ* locations (BD12—94°E, 10.3°N and BD14—88°E, 7°N) over the BoB for the period 2013–2014. Out of these two buoys,
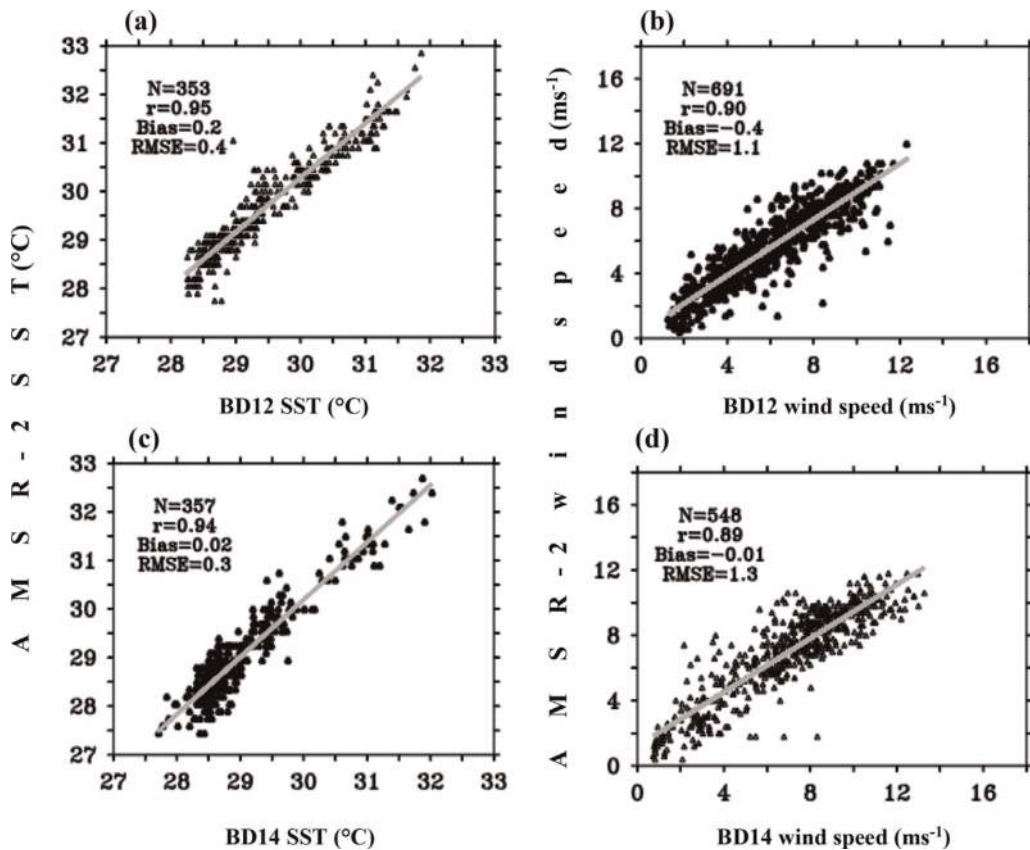
Figure 4.
Scatter plot analysis of AMSR-2 SST at (a) BD12—coastal region and (c) BD14—open ocean. (b) and (d) are same as (a) and (c) but for the wind speed during the period 2013–2014.

BD12 is situated near at the coastal region, i.e., east of the Andaman Island (~100–150 km) and the BD14 is placed in the open ocean, i.e., southern BoB region. **Figure 4** shows the statistical analyses of AMSR-2 SST and wind speed with respect to the *in-situ* observations. The formulations used in the present study are described in the Section 3.1. The SST statistics revealed that the BD12 and BD14 show an RMSE (Eq. (1)) error of 0.4 and 0.3°C (**Figure 4a** and **c**). Considering its correlation (r) and bias, BD12 (BD14) shows 0.95 (0.94) and 0.2°C (0.02°C), respectively (Eqs. (2) and (3)). It means that expected AMSR-2 accuracy is less towards the coastal region as compared to the open ocean. The similar statistics are conducted for the satellite derived wind speed. The results showed that an RMSE of 1.1 and 1.3 m s^{-1}, respectively, with a bias and correlation of 0.9 m s^{-1} and -0.4 (-0.02) at BD12 and BD14 locations (**Figure 5b** and **d**). However, all these obtained SST and wind speed errors are within the prescribed accuracy mentioned by the AMSR-2 (± 0.8°C and ± 1.5 m s^{-1}).

3.1 Statistical formulation used

A common set of mathematical and statistical techniques has been used to assess a performance of the AMSR-2 satellite measurements over the BoB region. It could further helpful to quantify the uncertainty and as well as for the rational use of the AMSR-2 information over the current region. The study employs the most widely used metrics such as bias, linear correlation and root mean square error, respectively. The formulas related to the error statistics are as follows.

$$RMSE = \sqrt{\frac{1}{n} \sum_{i=1}^{n}((x_i - x_{obs})/x_{obs})^2} \tag{1}$$

$$Bias = x_i - x_{obs} \tag{2}$$

$$correlation\ (r) = \frac{1}{n-1}\sum(x_i - \bar{x}/s_x)\ (y_i - \bar{y})/s_y) \tag{3}$$

where n, x_i, and x_{obs} represents the total number of samples, satellite and *in-situ* observations, respectively. $\bar{x}$ and $\bar{y}$ indicates the temporal mean of satellite and *in-situ* measurements and whereas s_x and s_y shows the standard deviation of it.

3.2 SST—wind speed relationship over the BoB

This section briefly explains the SST dependency on the surface wind speed over the BoB region (**Figure 5**). The analysis comprises of northern to southern BoB at different locations and scenarios such as eddy environment (BD08), near a coastal region (BD12) and open ocean areas (BD10 and BD14). Note that the SST-wind relationship is evaluated at BD08 location only during the WCE period. Because, the
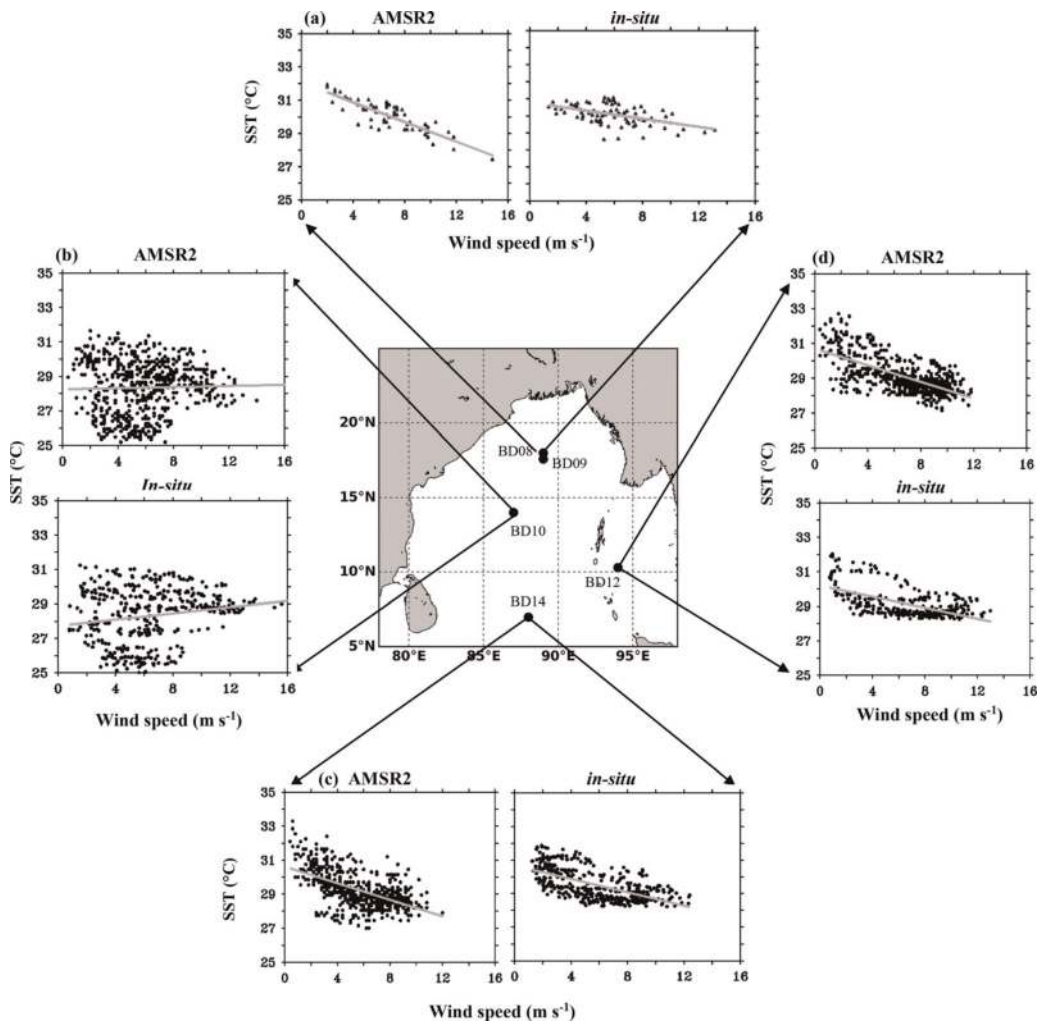

Figure 5.
Relationship between SST (°C) and wind speed (m s⁻¹) of AMSR-2 and in-situ measurements during (a) warm core eddy period (b and c) at BD10 and BD14—open ocean and (d) BD12—coastal region. Note that warm core eddy period considers only the BD08 observations.

estimated variations are minimal at both the BD08 and BD09 so the analysis related to the BD09 is excluded here. **Figure 5a** shows the SST-wind speed relation during the WCE period. The relationship shows a negative trend inferring that SST decreases with an increase in wind speed for both AMSR-2 and *in-situ* observations. The observed slope of the fitted line is high for the AMSR-2 with an SST difference of 3.4°C and is limited to 2°C in case of BD08. However, the long time period (2013–2014) analyses at the same location shows a contradictory relation indicating SST increases with an increase in wind speed [23]. **Figure 5b** shows the SST-wind speed relation over the central BoB region, i.e., BD10. Here, the relation displays a positive linear trend, addressing SST increases with an increase in wind speed [23]. Moreover, the deviation of SST and wind speed values of the fitted line is higher (lower) for the low (high) wind conditions. The data spread could be due to the fact that this region is active for the seasonal storms and monsoons. Considering the same relationship over the BD12 (eastern BoB) and BD14 (southern BoB), the SST decreases with an increase in wind speed (**Figure 5c** and **d**). It means that higher (lower) SST values are corresponding to the lower (higher) wind speed values. The present analysis also revealed that obtained AMSR-2 fitted line slope is relatively larger than the buoys fitted line. It could be due to the positive bias of SST and negative bias of wind speed over the BoB. In summary, satellite is underestimating the SST and wind speed variations because the ocean characteristics changes with the season and latitude over the BoB.

4. Conclusions

This chapter addresses the mesoscale warm core eddies and high-resolution products prominence in the Bay of Bengal. *In-situ* observations are used to analyze and quantify the errors of the AMSR-2 during the WCE over the northern BoB. The eddy has a life period of ~81 days with a 5° × 5° size. The statistical analysis of AMSR-2 SST with *in-situ* observations during the eddy period show an RMSE of 0.5–0.6°C. Interestingly, the obtained SST error is double that of the mean error calculated over the BoB region. In addition, the eddy impact on the overlying atmosphere is analyzed with showing an increase in the enthalpy fluxes and surface atmospheric parameter values. The similar event has been undertaken in the presence of AILA cyclone and the eddy role in the intensification process is observed. Briefly, Aila encounters the WCE on 24 May 2009 and after spending a few hours, it gets intensified into a severe cyclonic storm. The time series analysis of satellite and met-ocean parameters depicted that SLA and wind intensity shows its peak value of 20 cm and >45 knots after it passes through the WCE. Due to this sudden intensification, the coastal region receives a heavy rainfall (>18 mm day^{-1}) and strong winds (>45 knots) that led to the coastal inundation and flooding problems.

The AMSR-2 SST and wind speed parameters are evaluated qualitatively and quantitatively with respect to the buoy observations over the BoB. The statistical analysis of SST at BD12 and BD14 locations show an RMSE of 0.4 and 0.3°C and whereas wind speed shows an RMSE of 1.1 and 1.3 m s^{-1}, respectively. Along with this, the AMSR-2 SST and wind speed relationship is assessed in different aspects such as WCE, open and near coastal regions of the BoB. These analyses cover the whole BoB region and the obtained SST and wind speed interactions helpful to understand the air-sea interaction processes. The relationship exhibits a both linear positive and negative slopes over the BoB. It infers that wind speed and SST shows contrasting features within the BoB region. For example, BD08, BD12 and BD14 displays the negative relation inferring SST decreases with an increase in wind speed in both AMSR-2 and buoy observations. However, BD10 location shows the

opposite relation (i.e., positive relation) indicating SST increases with an increase in the wind speed. The overall results directed that AMSR-2 is able to replicate the buoy induced signals with positive bias in the SST and negative bias in the wind speed over the BoB.

Acknowledgements

Conflict of interest

The authors declare that they do not have any competing interests to publish this book chapter.

List of acronyms

AMSR-2	advanced microwave scanning radiometer-2
AVISO	archiving, validation, and interpretation of satellite oceanographic
BoB	Bay of Bengal
RMSE	root mean square error
SAT	surface air temperature
SLA	sea level anomalies
SST	sea surface temperature
TC	tropical cyclone
WCE	warm core eddy

Author details

Nanda Kishore Reddy Busireddy[1,2], Kumar Ankur[1] and Krishna Kishore Osuri[1*]

1 Department of Earth and Atmospheric Sciences, National Institute of Technology Rourkela, Odisha, India

2 Department of Earth, Atmospheric, and Planetary Sciences, Purdue University, West Lafayette, IN, USA

*Address all correspondence to: osurikishore@gmail.com

IntechOpen

References

[1] Patnaik KVKRK, Maneesha K, Sadhuram Y, Prasad KVSR, Ramana Murty TV, Brahmananda Rao V. East India Coastal Current induced eddies and their interaction with tropical storms over Bay of Bengal. Journal of Operational Oceanography. 2014;**7**(1): 58-68

[2] Murty TV, Rao MM, Sadhuram Y, Sridevi B, Maneesha K, Sujith Kumar S, et al. Objective mapping of observed sub-surface mesoscale cold core eddy in the Bay of Bengal by stochastic inverse technique with tomographically simulated travel times. Indian Journal of Geo-Marine Sciences. 2011;**40**:307-324

[3] Faghmous JH, Frenger I, Yao Y, Warmka R, Lindell A, Kumar V. A daily global mesoscale ocean eddy dataset from satellite altimetry. Scientific Data. 2015;**2**:150028

[4] Beron-Vera FJ, Wang Y, Olascoaga MJ, Goni GJ, Haller G. Objective detection of oceanic eddies and the Agulhas leakage. Journal of Physical Oceanography. 2013;**43**(7):1426-1438

[5] Gopalan AKS, Krishna VV, Ali MM, Sharma R. Detection of Bay of Bengal eddies from TOPEX and in situ observations. Journal of Marine Research. 2000;**58**(5):721-734

[6] Chen G, Wang D, Hou Y. The features and interannual variability mechanism of mesoscale eddies in the Bay of Bengal. Continental Shelf Research. 2012;**47**:178-185

[7] Kumar BP, Vialard J, Lengaigne M, Murty VSN, Mcphaden MJ. TropFlux: Air-sea fluxes for the global tropical oceans—Description and evaluation. Climate Dynamics. 2012;**38**(7-8): 1521-1543

[8] Goni GJ, Trinanes JA. Ocean thermal structure monitoring could aid in the intensity forecast of tropical cyclones. Eos, Transactions American Geophysical Union. 2003;**84**(51): 573-578

[9] Mainelli M, DeMaria M, Shay LK, Goni G. Application of oceanic heat content estimation to operational forecasting of recent Atlantic category 5 hurricanes. Weather and Forecasting. 2008;**23**(1):3-16

[10] Sadhuram Y, Maneesha V, Murty TVR. Intensification of Aila (May 2009) due to a warm core eddy in the north Bay of Bengal. Natural Hazards. 2012; **63**(3):1515-1525

[11] Oropeza F, Raga GB. Rapid deepening of tropical cyclones in the northeastern Tropical Pacific: The relationship with oceanic eddies. Atmosfera. 2015;**28**(1):27-42

[12] Hong X, Chang SW, Raman S, Shay LK, Hodur R. The interaction between Hurricane Opal (1995) and a warm core ring in the Gulf of Mexico. Monthly Weather Review. 2000;**128**(5): 1347-1365

[13] Wu CC, Lee CY, Lin II. The effect of the ocean eddy on tropical cyclone intensity. Journal of the Atmospheric Sciences. 2007;**64**(10):3562-3578

[14] Prasanna Kumar S, Muraleedharan PM, Prasad TG, Gauns M, Ramaiah N, De Souza SN, et al. Why is the Bay of Bengal less productive during summer monsoon compared to the Arabian sea. Geophysical Research Letters. 2002; **29**(24):88-81

[15] Bruce JG, Kindle JC, Kantha LH, Kerling JL, Bailey JF. Recent observations and modeling in the Arabian Sea Laccadive high region. Journal of Geophysical Research, Oceans. 1998;**103**(C4):7593-7600

[16] Frenger I, Gruber N, Knutti R, Münnich M. Imprint of Southern Ocean eddies on winds, clouds and rainfall. Nature Geoscience. 2013;**6**(8):608

[17] Dandapat S, Chakraborty A. Mesoscale eddies in the Western Bay of Bengal as observed from satellite altimetry in 1993–2014: Statistical characteristics, variability and three-dimensional properties. IEEE Journal of Selected Topics in Applied Earth Observations and Remote Sensing. 2016;**9**(11):5044-5054

[18] Busireddy NKR, Osuri KK, Sivareddy S, Venkatesan R. An observational analysis of the evolution of a mesoscale anti-cyclonic eddy over the Northern Bay of Bengal during May–July 2014. Ocean Dynamics. 2018; **68**(11):1431-1441

[19] Thadathil P, Muraleedharan PM, Rao RR, Somayajulu YK, Reddy GV, Revichandran C. Observed seasonal variability of barrier layer in the Bay of Bengal. Journal of Geophysical Research-Oceans. 2007;**112**(C2):1

[20] Nuncio M, Prasanna Kumar S. Evolution of cyclonic eddies and biogenic fluxes in the northern Bay of Bengal. Biogeosciences Discussions. 2013;**10**(10):16213-16236

[21] Chelton DB, Schlax MG, Samelson RM, de Szoeke RA. Global observations of large oceanic eddies. Geophysical Research Letters. 2007;**34**(15):p. L15606. DOI: 10.1029/2007GL030812

[22] Chen G, Hou Y, Chu X. Mesoscale eddies in the South China Sea: Mean properties, spatiotemporal variability, and impact on thermohaline structure. Journal of Geophysical Research, Oceans. 2011;**116**(C6):p.C06018

[23] Reddy BNK, Venkatesan R, Osuri KK, Mathew S, Kadiyam J, Joseph KJ. Comparison of AMSR-2 wind speed and sea surface temperature with moored buoy observations over the Northern Indian Ocean. Journal of Earth System Science. 2018;**127**(1):14

[24] Cyriac A, Ghoshal T, Shaileshbhai PR, Chakraborty A. Variability of sensible heat flux over the Bay of Bengal and its connection to Indian Ocean Dipole events. Ocean Science Journal. 2016;**51**(1):97-107

[25] Gray WM. Global view of the origins of tropical disturbances and storms. Monthly Weather Review. 1968; **96**:669-700

[26] Niyogi D, Subramanian S, Osuri KK. The role of land surface processes on tropical cyclones: Introduction to Land Surface Models. In: Advanced Numerical Modeling and Data Assimilation Techniques for Tropical Cyclone Prediction. Dordrecht. Springer; 2016. pp. 221-246